Journal of Power Sources 223 (2013) 165–174

Contents lists available at SciVerse ScienceDirect

Journal of Power Sources

journal homepage: www.elsevier.com/locate/jpowsour

Surfactant-free electrochemical synthesis of hierarchical platinum particle electrocatalysts for oxidation of ammonia

Jie Liu [a], Wenbin Hu [a], Cheng Zhong [a,*], Y. Frank Cheng [b,**]

[a] State Key Laboratory of Metal Matrix Composites, Shanghai Jiao Tong University, Shanghai 200240, China
[b] Department of Mechanical & Manufacturing Engineering, University of Calgary, 2500 University Drive NW, Calgary, AB, Canada T2N 1N4

HIGHLIGHTS

- ► Fabricate hierarchical platinum (Pt) particle electrocatalysts for the ammonia oxidation.
- ► Characterize the activity of Pt electrocatalysts with a wide variety of morphologies.
- ► Develop the surfactant-free electrodeposition method for fabrication of Pt electrocatalysts.
- ► Understand the effect of the surface morphology of Pt electrocatalysts on their activity.

ARTICLE INFO

Article history:
Received 6 July 2012
Received in revised form
15 September 2012
Accepted 18 September 2012
Available online 28 September 2012

Keywords:
Electrocatalysts
Oxidation of ammonia
Electro-deposition
Surface morphologies
Hierarchical platinum nanoparticles
Cyclic voltammetry

ABSTRACT

The platinum (Pt) particle electrocatalysts were fabricated by a surfactant-free, electro-deposition technique in the cyclic voltammetric mode for electro-oxidation of ammonia in aqueous solutions. The hierarchical Pt nanoparticles with various morphologies, including sheet-, flower-, prickly sphere- and cauliflower-like shapes, were obtained by controlling the electrodepositing parameters. The amount of Pt loading was determined by an inductively coupled plasma method, and the electrocatalytic activity of the prepared nano-Pt electrocatalysts for the ammonia oxidation was characterized by cyclic voltammetry. The results showed that there is a remarkable effect of the surface morphology of Pt particles on the electrocatalytic activity. In particular, the hierarchical Pt particles have a much higher electrocatalytic activity for the ammonia oxidation than the smooth, spherical Pt particles. The improved electrocatalytic activity is attributed not only to the large electrochemically active surface area (ECSA) achieved, but also to the high electrocatalytic activity per unit ECSA. Electro-deposition technique provides a promising alternative to fabricate high-performance electrocatalysts for oxidation of ammonia in aqueous solutions.

1. Introduction

Electro-oxidation of ammonia has been extensively studied in recent years for development of ammonia-based fuel cell technologies [1–4], production of hydrogen fuel [5–7], electrochemical decomposition of ammonia for environmental purpose [8–10], and fabrication of electrochemical sensors [11,12]. Platinum (Pt) has been so far recognized as the most effective electrocatalyst for the ammonia oxidation [13]. However, due to the financial non-affordability and the limited resources of Pt, it has not been used at an industrial scale yet. In the past decade, considerable effort has been devoted to development of high-performance electrocatalysts that are able to enhance effectively the kinetics of ammonia electro-oxidation, and simultaneously, reduce the Pt loading in the catalysts [3,4,6–12]. Since the performance of electrocatalysts depends strongly on their surface morphology [14–18], attention has been paid to fabricate Pt electrocatalysts with various morphologies in order to improve the electrocatalytic activities and, simultaneously, reduce cost.

It was reported [19–24] that the hierarchically structured micro- and nano-materials, fabricated upon various nano-structured units, such as nano-particles, nano-rods and nano-sheets, show a high performance in electrocatalysis. The methods used to prepare these complex hierarchical micro- and nano-structures include solvothermal or hydrothermal route [23,25], microemulsion [26], microwave irradiation and template growth [27–29]. Most of them require various surfactants, organic additives or templates. However,

* Corresponding author. Tel./fax: +86 21 34202981.
** Corresponding author. Tel.: +1 403 220 3693; fax: +1 403 282 8406.
E-mail addresses: chengz@sjtu.edu.cn (C. Zhong), fcheng@ucalgary.ca (Y.F. Cheng).

0378-7753/$ – see front matter © 2012 Elsevier B.V. All rights reserved.
http://dx.doi.org/10.1016/j.jpowsour.2012.09.074

addition of surfactants introduces heterogeneous impurities, potentially affecting the performance of electrocatalysts. Moreover, post-treatments are required to remove these organic additives or templates from the fabricated electrocatalysts. This could destroy the prepared hierarchical structure [30]. Therefore, it has remained a technical challenge to develop surfactant-free techniques for fabrication of hierarchical micro- and nano-structured electrocatalysts.

Electro-deposition technique has unique advantages, such as a high purity of deposit, easy-to-control procedure and low cost of implementation [31,32], over other methods to prepare the hierarchical nano-structures. For example, Guo et al. [19] used electro-deposition to prepare diameter-controlled, hierarchical, flower-like Au micro-structures. Similar hierarchical, flower-like noble metal particles have also been prepared by electro-deposition [33–35].

To date, there has been limited work to prepare Pt particles with various hierarchical structures by electro-deposition. Effects of the electrodepositing parameters on the hierarchical structure have remained unclear. Furthermore, the morphological effect of the hierarchical Pt particles on the ammonia electro-oxidation has not been investigated.

This work was aimed to develop an electrochemical method to prepare hierarchical Pt particles, with a low Pt loading while achieving a high electrocatalytic activity for oxidation of ammonia. The Pt particle electrocatalyst was prepared on an indium tin oxide (ITO) substrate by electro-deposition technique. The hierarchical Pt particles with various surface morphologies, including sheet-, flower-, prickly sphere- and cauliflower-like ones, were obtained in the absence of any organic additive. The amount of Pt loading was determined by an inductively coupled plasma (ICP) method, and the effect of surface morphology of the hierarchical Pt particles on their electrocatalytic activity for the ammonia oxidation in alkaline solutions was characterized by cyclic voltammetry (CV) and scanning electron microscopy (SEM) observation. It is anticipated that this work provides an insight into development of economically affordable, high-performance Pt electrocatalysts for the ammonia oxidation.

2. Experimental

2.1. Preparation of Pt electrocatalysts

Electro-deposition of Pt particles was performed by using a PARSTAT 2273 potentiostat/galvanostat, and an ITO was used as working electrode (WE), a Pt plate as counter electrode (CE), and a saturated calomel electrode (SCE) as reference electrode (RE). Pt particles were electrodeposited on the ITO substrate with an exposed area of 1 cm^2 under cyclic voltammetric condition as shown in Fig. 1. The upper potential limit (E_U) was 0.6 V(SCE), and the lower potential limit (E_L) was between 0 and −0.6 V(SCE). The potential scanning rate (ν) was ranged from 0.05 to 20 V s^{-1}. Prior to electro-deposition, the ITO glasses were cleaned in acetone and ultrapure water by sonication, and dried with a nitrogen steam.

The depositing electrolyte contained 0.5 mol L^{-1} H_2SO_4, 5×10^{-3} mol L^{-1} H_2PtCl_6 and distilled water (ultra-high purity, 18 MΩ cm in resistivity). All chemicals used were the analytic grade reagents.

2.2. Characterization of morphology and the Pt loading amount of electrocatalysts

The surface morphology of the prepared Pt electrocatalysts was characterized using a SEM (Quanta FEG250).

The amount of Pt in the prepared electrocatalyst, i.e., Pt loading, was determined by an ICP (Thermo Scientific, iCAP 6000 series) after dissolving Pt from the substrate. The Pt loading (μg cm^{-2}) is normalized by the geometric area of the working electrode.

2.3. Characterization of the electrocatalytic activity of Pt electrocatalysts

The electrocatalytic activity of the prepared Pt electrocatalysts for the ammonia oxidation was characterized by CV measurements. The solution contained 0.1 mol L^{-1} ammonia and 1 mol L^{-1} KOH. A three-electrode cell was used, with the Pt electrocatalyst as WE, a platinum plate as CE and a SCE as RE. The CVs were measured at a potential sweep rate of 0.01 V s^{-1}. The static electrode was used in this work in order to be comparable to the published work in this area [4–12], where the ammonia electro-oxidation testing was conducted on stationary electrodes. The electrochemically active surface area (ECSA, cm^2 cm^{-2}) of Pt electrocatalysts was evaluated from the steady-state CVs recorded at 0.05 V s^{-1} in 0.5 mol L^{-1} H_2SO_4 solution, and its value was normalized by the geometric area of the working electrode. The solution was deaerated by purging a high-purity Ar gas (99.999%) throughout the test. All tests were carried out at 25 ± 1 °C. Each test was repeated five times and the standard deviation of the obtained results was calculated and shown as error bar in the figures.

3. Results

3.1. Surface morphology of prepared Pt nano-particle electrocatalysts

Fig. 2 shows the SEM images of surface morphology of the prepared Pt electrocatalysts by cyclic voltammetric deposition at a scan rate of 0.05 V s^{-1} with various E_L ranging from 0 to −0.6 V(SCE).

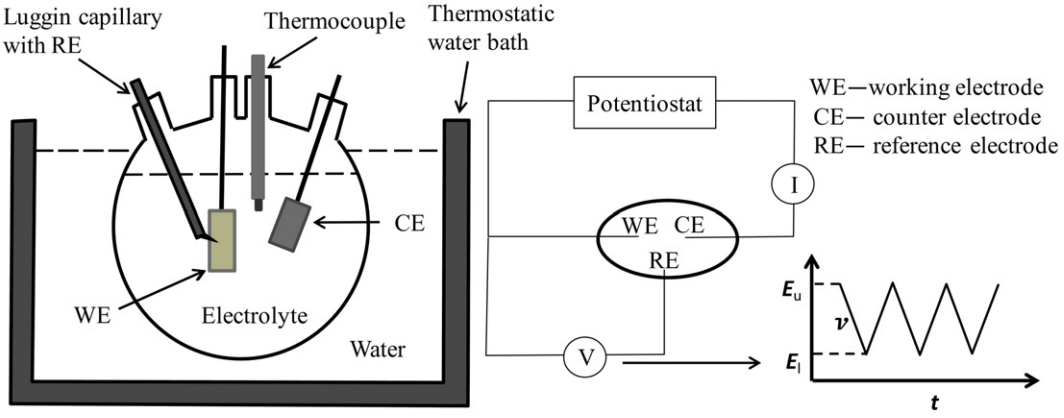

Fig. 1. Experimental set-up and the waveform used in electro-deposition, where E_U and E_L are the upper and lower potential limits, and ν is the scan rate.

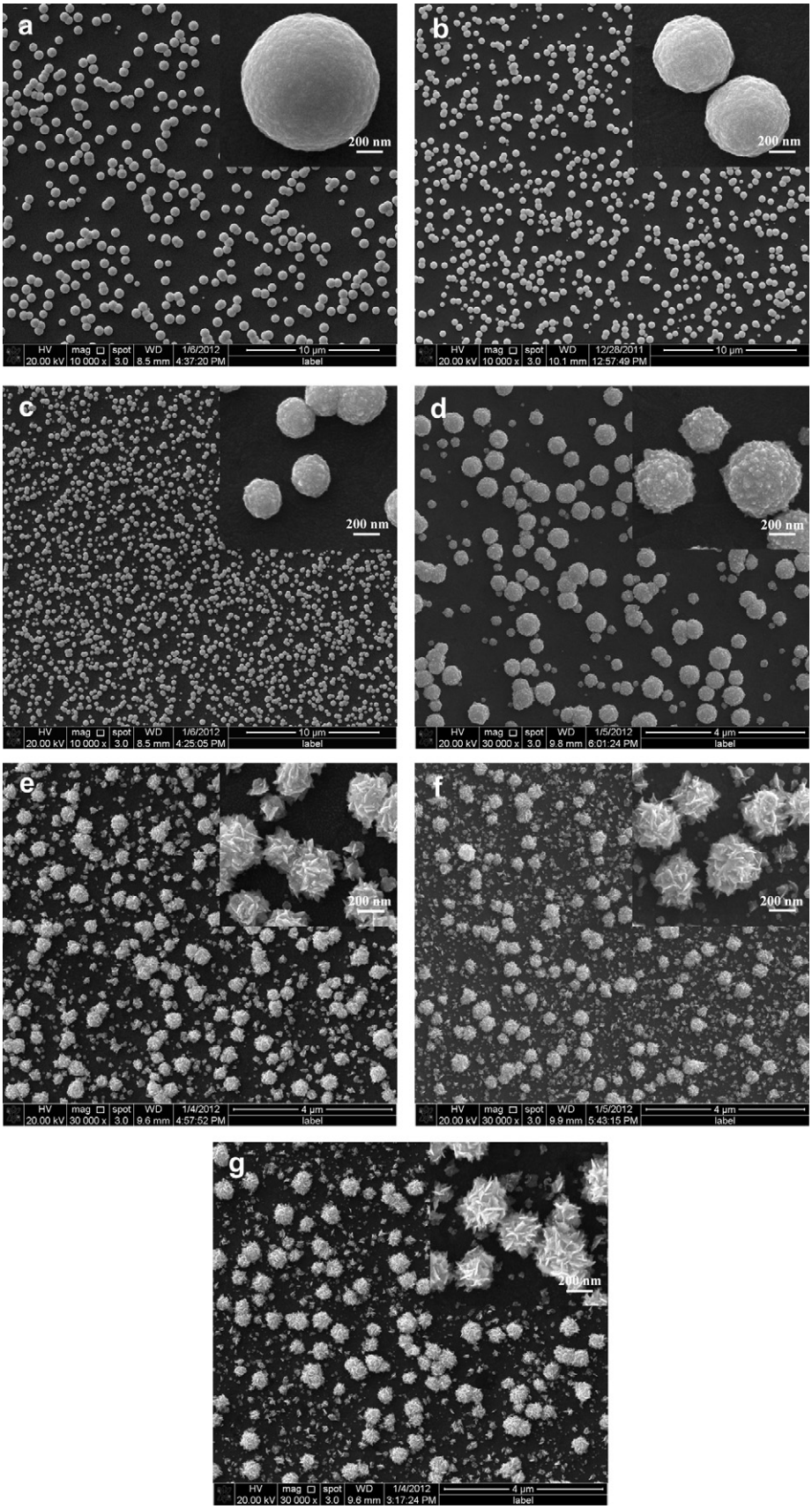

Fig. 2. SEM images of the surface morphology of Pt electrocatalysts prepared at the scan rate of 0.05 V s^{-1} with various E_L (a) 0, (b) −0.1, (c) −0.2, (d) −0.3, (e) −0.4, (f) −0.5 and (g) −0.6 V(SCE).

The bright dots in the pictures refer to the deposited Pt particles. It is seen that the morphology of the deposited Pt particles changes remarkably with E_L. When E_L is less negative, i.e., 0 to −0.1 V(SCE), the Pt particles are featured with a spherical shape with a smooth surface, as seen in Fig. 2a and b. The enlarged images inserting in Fig. 2a and b show that the spherical Pt particles actually consist of a large number of agglomerate small Pt particles. When E_L is shifted negatively to −0.2 and −0.3 V(SCE), the surface of the Pt particles become somewhat nano-roughened (Fig. 2c and d). Higher magnification images reveal that there are many protruding tips existing on the surface of Pt particle. As E_L further decreases to −0.4 and −0.6 V(SCE), the prepared Pt particles are shaped with a hierarchical, flower-like morphology (Fig. 2e–g), and the flower-like Pt particles consist of a large number of petal-like nano-sheets with a thickness of about 10 nm (inset in Fig. 2g).

Fig. 3 shows the SEM images of surface morphology of the prepared Pt electrocatalysts deposited at E_L of −0.1 V(SCE), but at various scan rates. With the increment of scan rate, the number density of Pt particles decreases while the size of the Pt particles increases slightly. Compared to E_L, there is no apparent effect of scan rate on the morphology of Pt particles, all of which are featured with a spherical shape.

Fig. 4 shows the SEM images of the morphology of Pt electrocatalysts deposited at E_L of −0.6 V(SCE) at various scan rates. Apparently, the morphology of Pt particles is quite different from those in Fig. 3. Pt particles fabricated at lower E_L are featured with a complex 3D hierarchical morphology. Furthermore, it is interesting to notice that scan rate plays an important role in the surface morphology of Pt particles. At low scan rates of 0.05 and 0.5 V s^{-1}, the Pt particles exhibit a hierarchical flower-like structure assembled by nano-sheets as building blocks (Fig. 4a and b). With the scan rate increases to 5 V s^{-1}, Pt particles exhibit prickly sphere-like morphology as seen in Fig. 4c. When the scan rate is 20 V s^{-1}, cauliflower-like Pt particles are observed (Fig. 4d).

3.2. Electrocatalytic activity of Pt particles for the ammonia oxidation

Fig. 5a shows the CVs measured on Pt electrocatalysts prepared at various depositing E_L with a scan rate of 0.05 V s^{-1} in 0.1 M ammonia + 1 M KOH solution. It is seen that there is a similar feature for all CV plots, i.e., an anodic current peak observed around −0.3 V(SCE), which is attributed to oxidation of ammonia [36,37]. Moreover, in the authors' previous work [37], CV is measured in the absence of ammonia, and there is no this characteristic current peak observed in the plot. Moreover, the peak current density depends strongly on the depositing E_L. For example, the peak current density measured on Pt electrocatalyst that is deposited at E_L of −0.6 V(SCE) with 55.5 μg cm^{-2} Pt loading is 2.6 mA cm^{-2}, which is much higher than that of 1.2 mA cm^{-2} on Pt electrocatalyst deposited at E_L of 0 V(SCE) with a higher Pt loading of 63.1 μg cm^{-2}.

Fig. 5b and c shows the CVs measured on Pt electrocatalysts deposited at E_L of −0.1 V(SCE) and −0.6 V(SCE), respectively, at various scan rates in 0.1 M ammonia + 1 M KOH solution. Generally, the peak current density increases with the amount of Pt loading. Furthermore, the peak current density for Pt electrocatalyst deposited at −0.6 V(SCE) is higher than that deposited at −0.1 V(SCE), indicating that the former has a higher electrocatalytic activity than the latter.

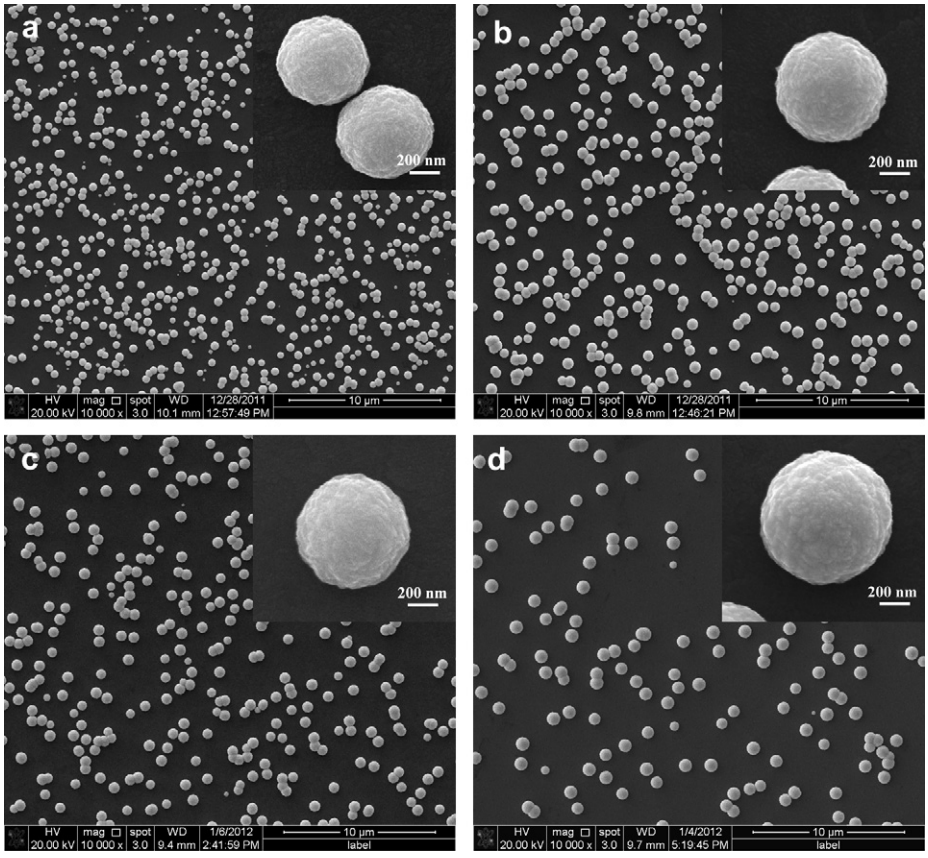

Fig. 3. SEM images of the surface morphology of Pt electrocatalysts prepared at E_L of −0.1 V(SCE) at various scan rates (a) 0.05, (b) 0.5, (c) 5 and (d) 20 V s^{-1}.

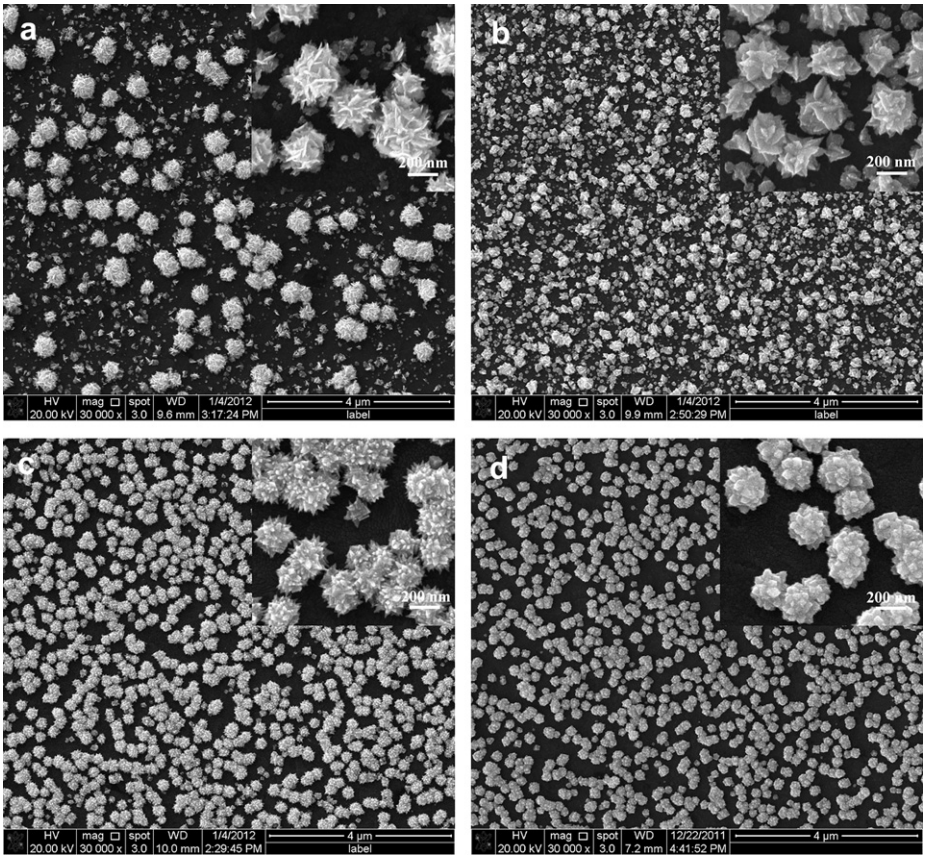

Fig. 4. SEM images of the surface morphology of Pt electrocatalysts prepared at E_L of −0.6 V(SCE) at various scan rates (a) 0.05, (b) 0.5, (c) 5 and (d) 20 V s^{-1}.

4. Discussion

4.1. Effects of electrodepositing conditions on surface morphology of Pt electrocatalysts

The present work demonstrates that it is feasible to fabricate hierarchical Pt particles with a wide variety of morphologies by controlling the electrodepositing potential and scanning rate. At a fixed scan rate of 0.05 V s^{-1}, as E_L shifts negatively from 0 to −0.6 V(SCE), the morphology of the deposited Pt particles changes from smooth, spherical shape (Fig. 2a and b) to those with a prickly sphere-like morphology (Fig. 2d), and finally to hierarchical flower-like Pt particles assembled by nano-sheets as building blocks (Fig. 2e–g). The morphological evolution is associated with the change of electrodepositing overpotential. During electrodeposition, the mass transport of Pt ions from the bulk solution toward the electrode surface (diffusion process) and the reduction of Pt ions (activation process) coexist [18]. For cyclic voltammetric electrodeposition, the reduction of Pt ions and the following nucleation and growth of Pt nuclei occur at the cathodic half-cycle. At less negative E_L, e.g., 0 to −0.1 V(SCE), a limited cathodic current is generated for the Pt reduction. Thus, the Pt depositing kinetics is activation-controlled, and the formed Pt particles show a densely agglomerate structure, i.e., the big spherical particle consists of a large number of small Pt particles, as seen in Fig. 2a and b. With E_L shifts negatively, the electrochemical reduction of Pt ions is enhanced, and the diffusion process cannot be neglected. The nucleation and growth of Pt is mixed-controlled by charge-transfer and diffusion processes. Generally, the diffusion-control process results in a dendrite growth feature [18,38,39]. As a consequence, the protruding points on Pt surface grow faster than other area, forming Pt particles with the prickly sphere-like surface morphology (Fig. 2d). As E_L further shifts negatively to −0.4 V(SCE) and −0.6 V(SCE), a large number of Pt ions are reduced in a short time period under the high cathodic overpotential. The Pt deposition process is now completely diffusion-controlled. The Pt nuclei tend to show a 2D planer growth mode, leading to formation of nano-sheets. The edges of the sheet grow much faster than other parts (Fig. 2e–g).

Furthermore, it is worth noticing that the effect of scan rate during electrodeposition on morphology of Pt particles depends on the value of E_L. When E_L is less negative, such as −0.1 V(SCE), Pt particles are characterized with a spherical feature at all scan rates (Fig. 3). However, scan rate affects greatly the morphology of Pt particles deposited at a more negative E_L of −0.6 V(SCE) (Fig. 4). This would be attributed to the competitive effect between the activation and diffusion processes. Fig. 6 is the schematic diagram of a two-dimensional map showing the particle morphologies which are dependent on scan rate and the voltage difference. During the cathodic half-cycle of electrodeposition, Pt ions are consumed due to electro-reduction, while diffusion of Pt ions from the bulk solution to cathode compensates the depletion. When the Pt ion consumption rate is higher than the diffusion rate, a Pt ion depletion layer is formed, affecting the growth of Pt nuclei. At less negative E_L, the consumed Pt ions can be timely supplied, and there is no obvious depletion layer formed during the cathodic half-cycle. The growth of Pt deposits is always dominated by the activation-control process irrespective of the scan rate. Thus, there is no obvious effect of scan rate on the electrodeposition process, and the formed Pt particles are always shaped as smooth spherical

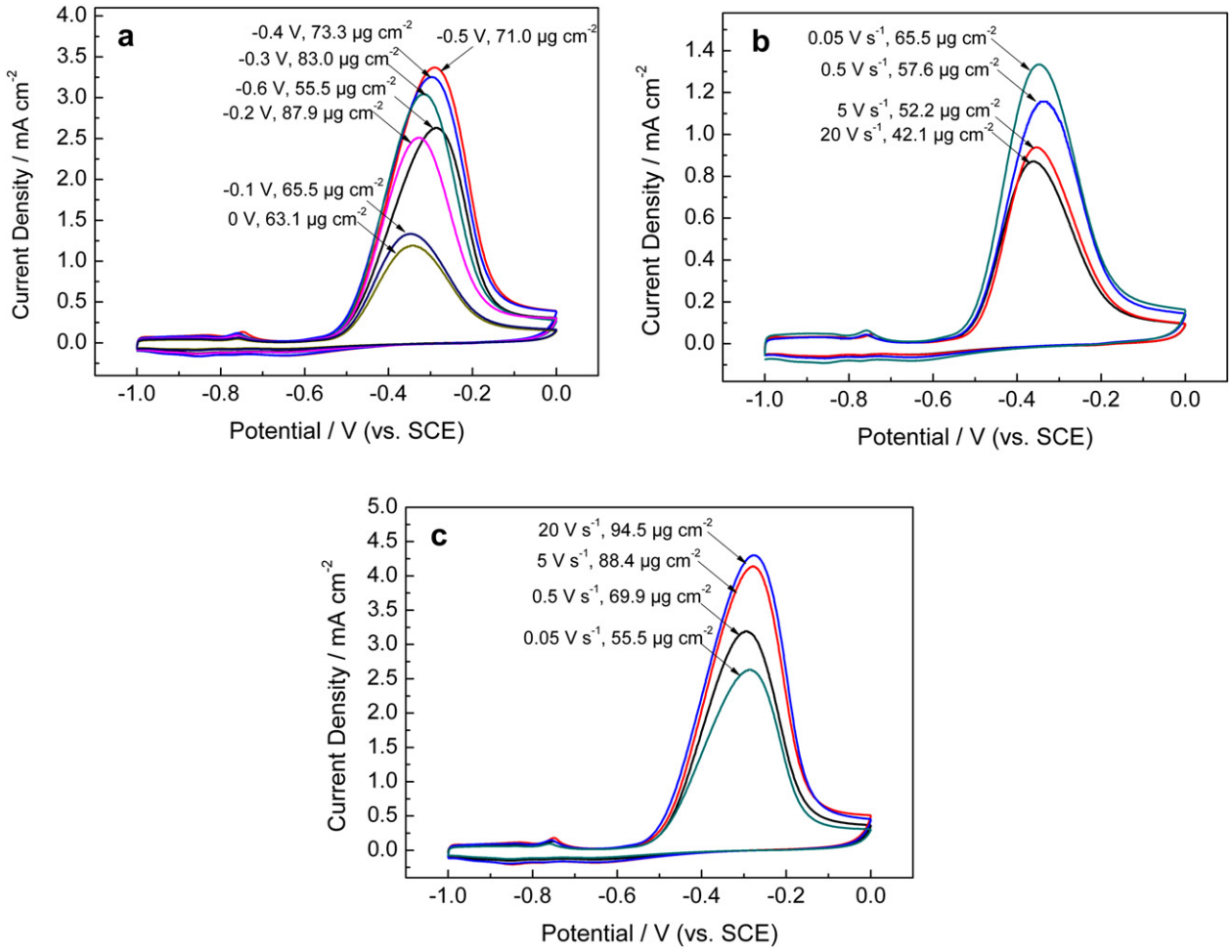

Fig. 5. Cyclic voltammograms measured on Pt electrocatalysts prepared at (a) various E_L and the scan rate of 0.05 V s^{-1}, and various scan rates at E_L of (b) −0.1 V(SCE) and (c) −0.6 V(SCE) in 1 M KOH and 0.1 M ammonia solution.

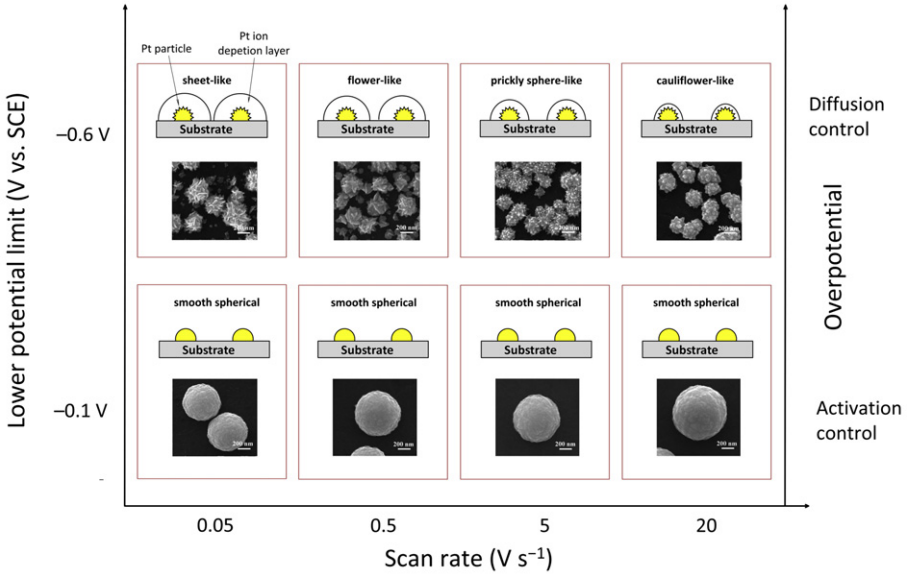

Fig. 6. Schematic diagram of a two-dimensional map showing the particle morphologies which are dependent on scan rate and the voltage difference.

morphology (Fig. 3). However, at more negative E_L, the Pt ion reduction rate is much higher than the diffusion rate. As a result, a Pt ion depletion layer would be formed during the cathodic half-cycle. This makes the electrodeposition process change to diffusion-controlled. During the anodic half-cycle, the reduced, consumed Pt ions at the electrode surface are replenished. Thus, the anodic half-cycle would decrease the thickness or even eliminate the Pt depletion layer. This strongly facilitates the Pt ion transport, and enables a low degree of mass transfer limitations. Previous studies on pulse electrodeposition found that the value of pulse frequency (f) plays an important role in determining the average thickness of the diffusion-boundary layer, δ_p, which is related to the mass transport of metal ions in the solution [38,40,41]. The value of δ_p decreases with the reciprocal of $f^{1/2}$ [41]. For example, on Pt, δ_p decreases from about 10^{-3} cm at f of 0.025 kHz to about 10^{-4} cm at f of 1 kHz. This makes the overall process change from diffusion controlled to activation controlled [38,40]. The similar phenomenon would also be expected in the present work, i.e., the thickness of the diffusion-boundary layer decreases with the increasing scan rate. Therefore, Pt particles with various hierarchical structures, such as sheet-, prickly sphere- and cauliflower-like ones, can be formed (Fig. 4), depending on the degree of diffusion control achieved. In particular, the sheet-like morphologies (Fig. 4a) are obtained under a completely diffusion-controlled depositing condition, while the cauliflower-like (Fig. 4d) morphology is the characteristic with a mixed activation and diffusion controlled process.

4.2. Effect of electrodepositing conditions on the electrocatalytic activity of Pt electrocatalysts

The mechanism of ammonia electrooxidation on Pt proposed by Gerischer and Mauerer [42] involves the dehydrogenation step of $NH_{3,ads}$ to N_{ads} and the recombination of two $NH_{x,ads}$, where partially dehydrogenated species of $NH_{2,ads}$ and NH_{ads} are active intermediates to give the final product of N_2:

$$NH_3(aq) \rightarrow NH_{3,ads} \quad (1)$$

$$NH_{3,ads} + OH^- \rightarrow NH_{2,ads} + H_2O + e^- \quad (2)$$

$$NH_{2,ads} + OH^- \rightarrow NH_{ads} + H_2O + e^- \quad (3)$$

$$NH_{x,ads} + NH_{y,ads} \rightarrow N_2H_{x+y,ads} \quad (4)$$

$$N_2H_{x+y,ads} + (x+y)OH^- \rightarrow N_2 + (x+y)H_2O + (x+y)e^- \quad (5)$$

$$NH_{ads} + OH^- \rightarrow N_{ads} + H_2O + e^- \quad (6)$$

where $x = 1$ or 2 and $y = 1$ or 2.

The product of the ammonia electrodeposition on bulk Pt [13,14], Pt black [11,15], electrodeposited Pt [16] and Pt micro- and nano-particles [17,18] in alkaline solutions have been characterized by electrochemical mass spectrometry and surface-enhanced Raman spectroscopy. It was found that there is similar product generated on all of these electrodes. At mild anodic potentials, ammonia is fully oxidized to N_2. At more anodic potentials at which water is oxidized, a surface oxide is formed on Pt, where N_2 evolution is possible, accompanying with the simultaneous production of O_2 and nitrogen oxides, e.g., NO and N_2O. Considering the potential range used in this work, it is reasonable to assume that ammonia is fully oxidized to N_2 under the investigated condition. The anodic current peak in Fig. 5 is probably the overlapped characteristic peaks of the proposed oxidation reactions.

The electrocatalytic activity of Pt for oxidation of ammonia can be determined by Q_{AOR}/L_{Pt}, where Q_{AOR} is the charge required for the ammonia oxidation reaction (mC cm^{-2}) and L_{Pt} is the amount of Pt loading in the electrocatalyst. The value of Q_{AOR} is determined from the area integrated under the anodic current peak in CV. Fig. 7a shows the electrocatalytic activity expressed as Q_{AOR}/L_{Pt} of Pt electrocatalysts at various E_L at a scan rate of 0.05 V s^{-1}. It is seen that the electrocatalytic activity increases with the negative shift of E_L. For example, the Q_{AOR}/L_{Pt} of Pt electrocatalyst deposited at $E_L = -0.6$ V(SCE) is about 0.92 mC μg^{-1}, which is 2.5 times higher than that at E_L of 0 V(SCE). As analyzed, the effect of E_L on the electrocatalytic activity of Pt is associated with surface morphology of the deposited Pt particles. Electrodeposition at more negative E_L results in formation of Pt particles with a dendrite, hierarchical feature, with high electrocatalytic activities. Conversely, the smooth spherical Pt particles obtained at less negative E_L have the lowest electrocatalytic activity.

Fig. 7b shows the electrocatalytic activity of Pt electrocatalysts prepared at different scan rates at E_L of −0.1 V(SCE) and −0.6 V(SCE), respectively. It is seen that Pt particles prepared at low E_L shows a high electrocatalytic activity. The Q_{AOR}/L_{Pt} of Pt particles obtained at E_L of −0.1 V(SCE) is about 0.36–0.40 mC μg^{-1}, while that of the hierarchical Pt particles obtained at −0.6 V(SCE) shows a high value from 0.88 to 0.95 mC μg^{-1}. To understand mechanistically the effect of the morphological feature of Pt on

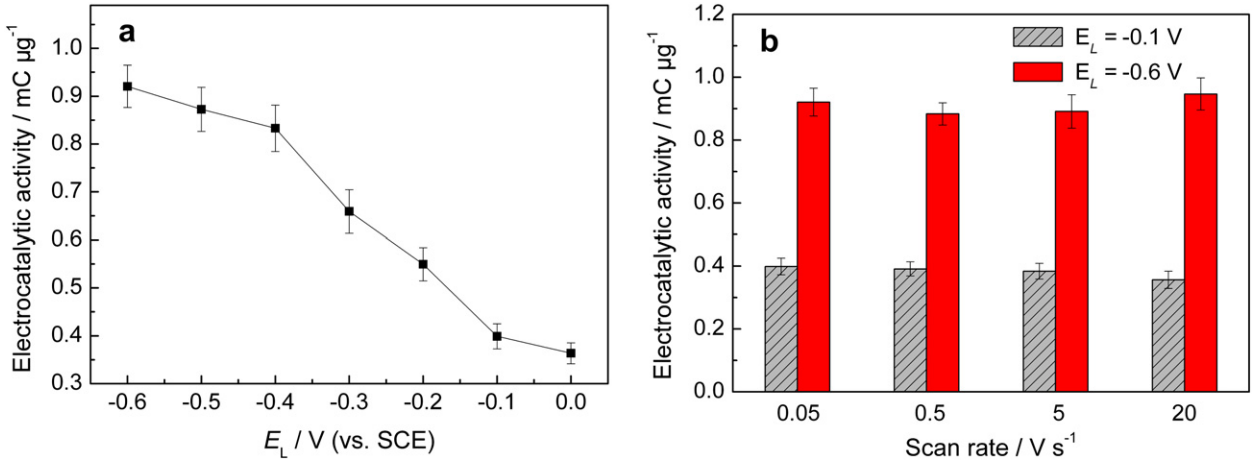

Fig. 7. Electrocatalytic activity of Pt electrocatalysts prepared at (a) various E_L and scan rate of 0.05 V s^{-1} and (b) various scan rates and E_L of −0.1 V(SCE) and −0.6 V(SCE).

its electrocatalytic activity, the electrochemically active surface area of Pt electrocatalysts is analyzed as follows.

4.3. Electrochemically active surface area of Pt electrocatalysts

The ECSA of the prepared Pt electrocatalyst is determined by measurements of CV in 0.5 M H_2SO_4. Fig. 8a shows the CVs measured on Pt electrocatalysts prepared at various E_L and the scan rate of 0.05 V s^{-1}. All CVs show typical potential regions for hydrogen adsorption/desorption at −0.2–0 V(SCE), and the formation/reduction of Pt oxide (Pt−OH_{ad}) at 0.5–1.0 V(SCE). The hydrogen desorption peaks at about −0.14 V(SCE) and −0.04 V(SCE) in the anodic branch are attributed to desorption of the weakly and strongly bonded hydrogen species, respectively [43]. Fig. 8b and c shows the CVs measured on Pt electrocatalysts deposited at various scan rates at E_L of −0.1 V(SCE) and −0.6 V(SCE), respectively. It is seen that Pt particles electrodeposited at lower E_L shows a much higher hydrogen adsorption/desorption current density than that deposited at higher E_L.

The ECSA (cm^2 cm^{-2}) of Pt electrocatalysts is calculated from CV by [44]:

$$\mathrm{ECSA} = \frac{Q_H}{Q_H^0} \tag{7}$$

where Q_H is the charge for hydrogen desorption (mC cm^{-2}), and Q_H^0 is the specific charge for a hydrogen monolayer on Pt (0.21 mC cm^{-2}) [45]. The Q_H value for the individual electrocatalyst can be calculated by integrating the area covered by the hydrogen adsorption current peak, subtracting the contribution of the double-charge layer. Furthermore, the ECSA is normalized by the amount of Pt loading in electrocatalysts, which is defined as specific active surface area (SSA). Fig. 9a shows the SSA of Pt electrocatalysts deposited at various E_L and the scanning rate of 0.05 V s^{-1}. It is seen that the SSA increases with the negative shift of E_L, indicating that the SSA of Pt electrocatalysts increases as the morphology of Pt particles changes from smooth spherical shape to hierarchical, flower-like one. This is further confirmed by Fig. 9b, where the SSA of Pt electrocatalysts deposited at various scan rates at E_L of −0.1 V(SCE) and −0.6 V(SCE) is shown. Pt electrocatalysts prepared at E_L of −0.6 V(SCE) have higher SSA (0.11–0.12 cm^2 μg^{-1}) than that (0.09–0.10 cm^2 μg^{-1}) obtained at E_L of −0.1 V(SCE).

Furthermore, SSA is not the single factor determining the electrocatalytic activity of Pt particles. Fig. 10 shows the electrocatalytic activity per unit SSA of Pt particles with different morphologies obtained at various scan rates at E_L of −0.1 V(SCE) and −0.6 V(SCE), respectively. It is clear that the electrocatalytic activity per unit SSA of the smooth, spherical Pt particles deposited at E_L of −0.1 V(SCE) is much lower than that of the hierarchical Pt particles obtained at E_L of −0.6 V(SCE). This indicates that the high electrocatalytic activity of the hierarchical Pt is attributed not only to the large SSA, but also to the high electrocatalytic activity per unit SSA. From the SEM images of the prepared hierarchical Pt particles (Fig. 4), they are featured with porous structures, containing a significant

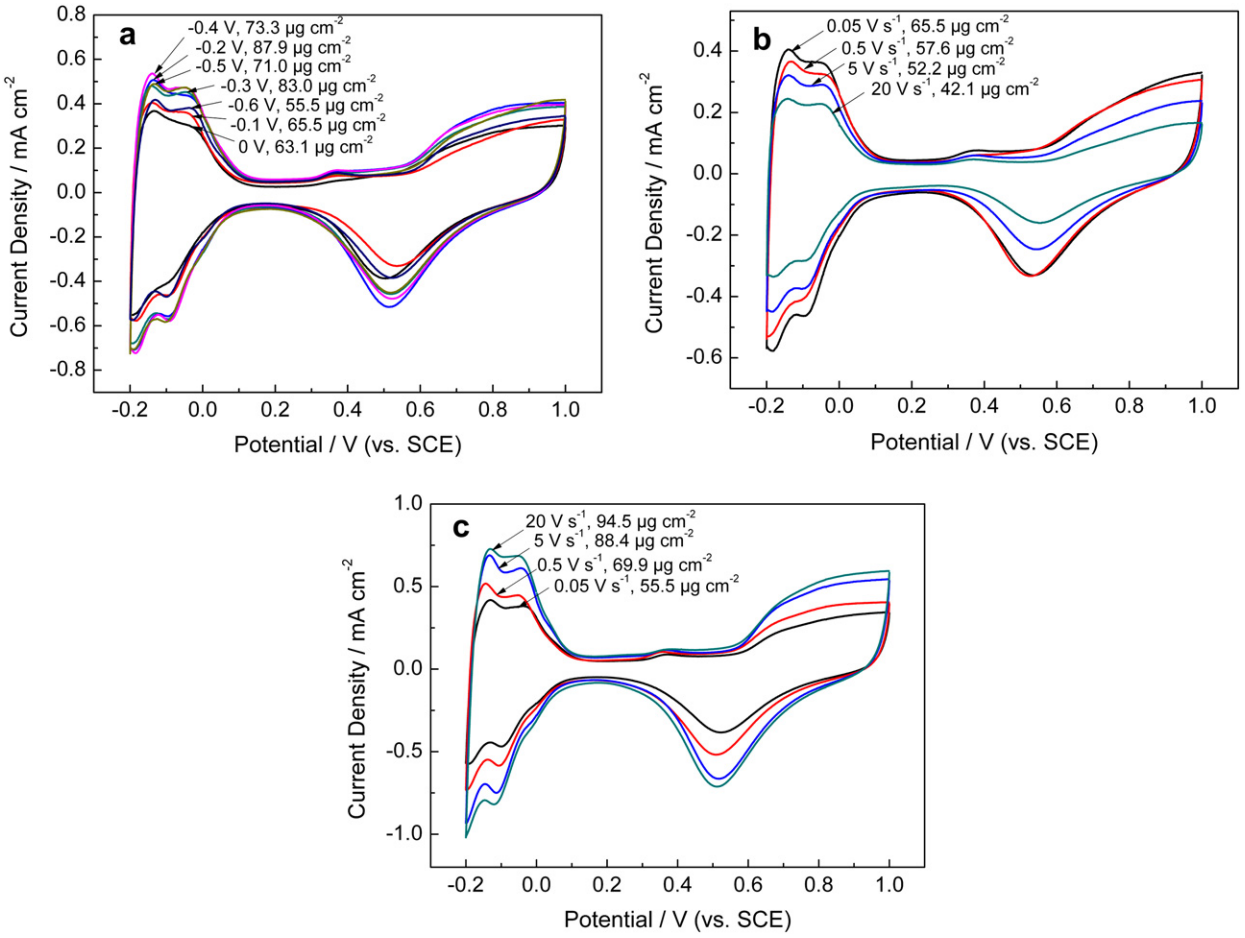

Fig. 8. Cyclic voltammograms measured on Pt electrocatalysts prepared at (a) various E_L and scan rate of 0.05 V s^{-1} and various scan rates for E_L of (b) −0.1 V(SCE) and (c) −0.6 V(SCE) in 0.5 M H_2SO_4 solution.

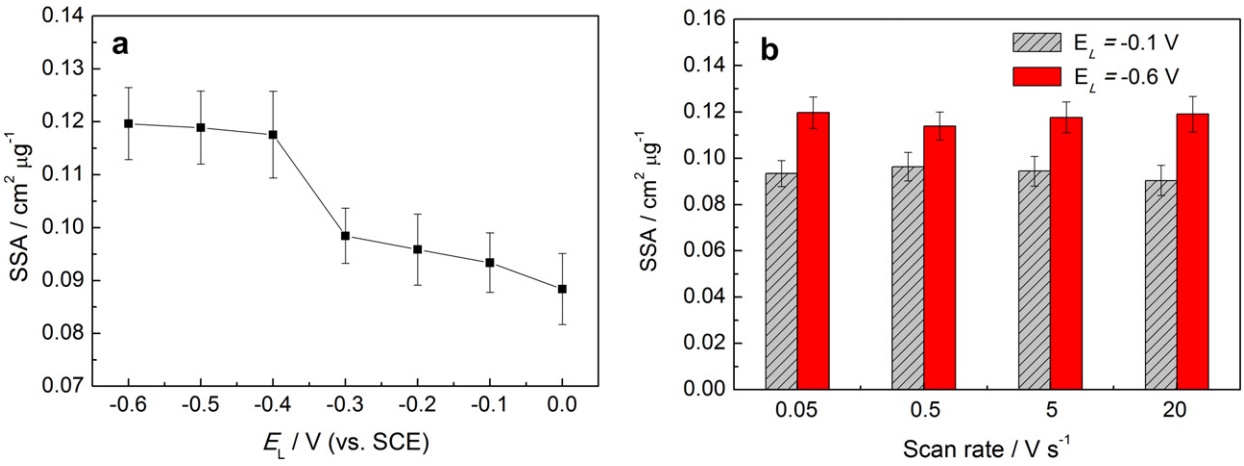

Fig. 9. SSA of Pt electrocatalysts prepared at (a) various E_L and the scan rate of 0.05 V s^{-1} and (b) various scan rates at E_L of −0.1 V(SCE) and −0.6 V(SCE).

number of protruding tips and edges on the surface. This could greatly contribute to the mass transport during reaction, leading to the higher electrocatalytic activity per unit SSA.

In the present work, the catalysts (Pt particles) were electro-deposited on a bulk electrode, and it is suitable for applications such as the production of hydrogen by ammonia electrolysis, and the electrochemical removal of ammonia and electrochemical sensors for ammonia analysis for the environmental purpose. In such applications, catalysts are usually electro-deposited on a chemically inert substrate. Present work demonstrates that, by controlling the electrodepositing mode and parameters, it is possible to enhance remarkably the activity of the prepared Pt catalysts.

With regard to the low temperature fuel cells applications, the Pt catalysts could be electro-deposited directly on a microporous carbon black anode of the cell. Previous work has shown that, although Pt catalysts prepared by electro-deposition generally have a large particle size than that prepared by other methods such as microemulsion, the electric field in the catalyst deposition enables the localization of Pt particles at the active reaction sites, which could lower the Pt loading. As demonstrated [20,21], although the size of Pt particles was about several hundreds of nm, they still exhibited a much higher activity compared to commercial Pt/C catalysts in fuel cell tests. It is thus believed that the catalyst performance will be further improved by decreasing the size of the particles prepared by electro-deposition. The further work will be carried out on electro-deposition of hierarchical Pt particles with small size on microporous carbon electrode for ammonia-based fuel cells applications.

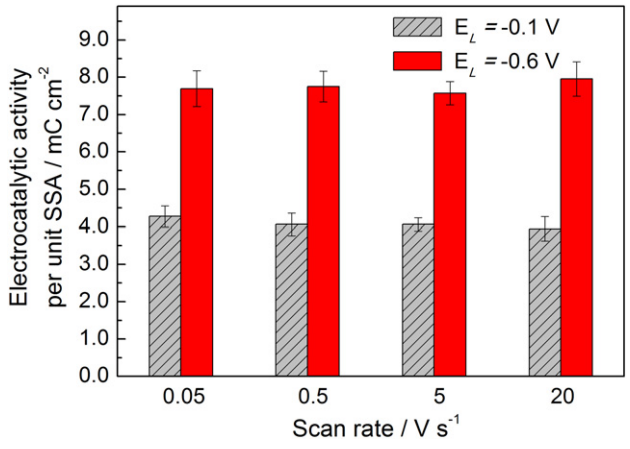

Fig. 10. Electrocatalytic activity per unit SSA of Pt particles with various morphologies prepared at various scan rates and E_L of −0.1 V(SCE) and −0.6 V(SCE).

5. Conclusions

The Pt particle electrocatalysts with various surface morphologies are prepared by electro-deposition on ITO substrate. As the lower limit of the cyclic depositing potential shifts negatively, the prepared Pt particles change from spherical to hierarchical, flower-like morphology. Furthermore, the hierarchical Pt particles with various morphologies, such as sheet-, flower-, prickly sphere- and cauliflower-like shape, can be fabricated by controlling the scan rate of the cyclic voltammetric deposition. The electrocatalytic activity of the prepared Pt electrocatalysts for the ammonia oxidation in aqueous solutions depends strongly on the surface morphology of Pt particles. The electrocatalytic activity of the hierarchical Pt particles is much higher than the smooth, spherical Pt particles, which is attributed not only to the high SSA, but also to its high electrocatalytic activity per unit SSA.

Acknowledgments

The authors thank Drs. W. Li, S. Xu and Y.J. Zhou of the Instrumental Analysis Center of Shanghai Jiao Tong University for the SEM and ICP analysis. This work was supported by the National Science Foundation for Distinguished Young Scholars of China (51125016), and partially supported by “Chen Guang” project supported by Shanghai Municipal Education Commission and Shanghai Education Development Foundation (11CG12), Research Fund for the Doctoral Program of Higher Education of China (20100073120109), Shanghai Jiao Tong University (IPP5124, IAP4063 and 1110248026) and Canada Research Chairs Program.

References

[1] C. Zamfirescu, I. Dincer, J. Power Sources 185 (2008) 459.
[2] S. Suzuki, H. Muroyama, T. Matsui, K. Eguchi, J. Power Sources 208 (2012) 257.
[3] F.J. Vidal-Iglesias, J. Solla-Gullón, V. Montiel, J.M. Feliu, A. Aldaz, J. Power Sources 171 (2007) 448.
[4] K. Endo, K. Nakamura, Y. Katayama, T. Miura, Electrochim. Acta 49 (2004) 2503.
[5] B.K. Boggs, G.G. Botte, J. Power Sources 192 (2009) 573.
[6] F. Vitse, M. Cooper, G.G. Botte, J. Power Sources 142 (2005) 18.
[7] L. Zhou, Y.F. Cheng, Int. J. Hydrog. Energy 33 (2008) 5897.
[8] F.J. Vidal-Iglesias, J. Solla-Gullón, V. Montiel, J.M. Feliu, A. Aldaz, J. Phys. Chem. B 109 (2005) 12914.

[9] E.P. Bonnin, E.J. Biddinger, G.G. Botte, J. Power Sources 182 (2008) 284.
[10] F.J. Vidal-Iglesias, N. García-Aráez, V. Montiel, J.M. Feliu, A. Aldaz, Electrochem. Commun. 5 (2003) 22.
[11] B.A. López de Mishima, D. Lescano, T. Molina Holgado, H.T. Mishima, Electrochim. Acta 43 (1998) 395.
[12] E. Moran, C. Cattaneo, H. Mishima, B.A. López de Mishima, S.P. Silvetti, J.L. Rodriguez, E. Pastor, J. Solid State Electron. 12 (2008) 583.
[13] A.C.A. de Vooys, M.T.M. Koper, R.A. van Santen, J.A.R. van Veen, J. Electroanal. Chem. 506 (2001) 127.
[14] J. Liu, C. Zhong, Y. Yang, Y.T. Wu, A.K. Jiang, Y.D. Deng, Z. Zhang, W.B. Hu, Int. J. Hydrog. Energy 37 (2012) 8981.
[15] H. Jeon, J. Joo, Y. Kwon, S. Uhm, J. Lee, J. Power Sources 195 (2010) 5929.
[16] F.J. Vidal-Iglesias, J. Solla-Gullón, P. Rodríguez, E. Herrero, V. Montiel, J.M. Feliu, A. Aldaz, Electrochem. Commun. 6 (2004) 1080.
[17] Y. Liu, M.F. Chi, V. Mazumder, K.L. More, S. Soled, J.D. Henao, S.H. Sun, Chem. Mater. 23 (2011) 4199.
[18] C. Zhong, W.B. Hu, Y.F. Cheng, J. Power Sources 196 (2011) 8064.
[19] S.J. Guo, L. Wang, E.K. Wang, Chem. Commun. 30 (2007) 3163.
[20] Y. Xia, W.K. Zhang, H. Huang, J. Power Sources 196 (2011) 5651.
[21] Y.L. Wang, Y.Q. Zhao, C.L. Xu, J. Power Sources 195 (2010) 6496.
[22] C.G. Hu, X.S. He, C.H. Xia, J. Power Sources 195 (2010) 1594.
[23] R.J. Chimentão, I. Kirm, F. Medina, X. Rodríguez, Y. Cesteros, P. Salagre, J.E. Sueiras, Chem. Commun. 27 (2004) 846.
[24] P. Gao, M. Zhang, H. Hou, Q. Xiao, Mater. Res. Bull. 43 (2008) 531.
[25] T.D. Ewers, A.K. Sra, B.C. Norris, R.E. Cable, C.H. Cheng, D.F. Shantz, R.E. Schaak, Chem. Commun. 17 (2005) 514.
[26] S.K. Haram, A.R. Mahadeshwar, S.G. Dixit, J. Phys. Chem. 100 (1996) 5868.
[27] X.H. Xia, J.P. Tu, J.Y. Xiang, X.H. Huang, X.L. Wang, X.B. Zhao, J. Power Sources 195 (2010) 2014.
[28] H.L. Cao, Q. Gong, X.F. Qian, H.L. Wang, J.T. Zai, Z.K. Zhu, Cryst. Growth Des. 7 (2007) 425.
[29] W.F. Jia, J.R. Li, G.H. Lin, L. Jiang, Cryst. Growth Des. 11 (2011) 3822.
[30] H.P. Liang, H.M. Zhang, J.S. Hu, Y.G. Guo, L.J. Wan, C.L. Bai, Angew. Chem. Int. Ed. 43 (2004) 1540.
[31] C. Paoletti, A. Cemmi, L. Giorgi, R. Giorgi, L. Pilloni, E. Serra, M. Pasquali, J. Power Sources 183 (2008) 84.
[32] H. Kim, N.P. Subramanian, B.N. Popov, J. Power Sources 138 (2004) 14.
[33] H.M. Zhang, W.Q. Zhou, Y.K. Du, P. Yang, C.Y. Wang, Electrochem. Commun. 12 (2010) 882.
[34] L. Wang, S.J. Guo, J.F. Zhai, X.G. Hu, S.J. Dong, Electrochim. Acta 53 (2008) 2776.
[35] L. Su, W.Z. Jia, L.C. Zhang, C. Beacham, H. Zhang, Y. Lei, J. Phys. Chem. C 114 (2010) 18121.
[36] K. Endo, Y. Katayama, T. Miura, Electrochim. Acta 49 (2004) 1635.
[37] K. Yao, Y.F. Cheng, J. Power Sources 173 (2007) 96.
[38] J.L. Zubimendi, G. Andreasen, W.E. Triaca, Electrochim. Acta 40 (1995) 1305.
[39] W.C. Ye, J.F. Yan, Q.A. Ye, F. Zhou, J. Phys. Chem. C 114 (2010) 15617.
[40] A. Visintin, J.C. Canullo, W.E. Triaca, A.J. Arvia, J. Electroanal. Chem. 239 (1988) 67.
[41] A.R. Despic, K.I. Popov, J. Appl. Electrochem. 1 (1971) 275.
[42] H. Gerischer, A. Mauerer, J. Electroanal. Chem. 25 (1970) 421.
[43] N.M. Markovic, P.N. Ross, Surf. Sci. Rep. 45 (2002) 117.
[44] F. Gloaguen, J.M. Léger, C. Lamy, A. Marmann, U. Stimming, R. Vogel, Electrochim. Acta 44 (1999) 1805.
[45] E. Antolini, L. Giorgi, A. Pozio, E. Passalacqua, J. Power Sources 77 (1999) 136.